The Thermal decomposition of Ca(OH)2 polymorphs

Beaudoin, J. J.; Sato, T.; Tumidajski, P. J.

Publisher's version / Version de l'éditeur:

RILEM, 2nd International Symposium on Advances in Concrete Through Science and Engineering [Proceedings], pp. 1-15, 2006-09-01

NRC·CNRC Institute for Research in Construction
CNRC·NRC Institut de recherche en construction
http://irc.nrc-cnrc.gc.ca

The Thermal decomposition of Ca(OH)2 polymorphs

NRCC-46310

Beaudoin, J.J.; Sato, T.; Tumidajski, P.J.

A version of this document is published in / Une version de ce document se trouve dans : 2nd International Symposium on Advances in Concrete Through Science and Engineering, Québec City, Sept. 11-13, 2006, pp. 1-15

THE THERMAL DECOMPOSITION OF $Ca(OH)_2$ POLYMORPHS

James J. Beaudoin (1), Taijiro Sato (1) and Peter J. Tumidajski (2)

(1) Institute for Research in Construction, National Research Council, Canada

(2) Centre for Advanced Building Technologies, The City College, George Brown, Canada

Abstract

The thermal decomposition of different polymorphs of $Ca(OH)_2$ with varying degrees of crystallinity and surface area was investigated. The nitrogen surface area values ranged from 3.7 to 31.1 m^2/g. The presence of two separate and distinct thermal decomposition events was observed depending on the degree of crystallinity. Binary mixtures of $Ca(OH)_2$ with substantially different degrees of crystallinity exhibited well defined thermal decomposition doublets. In addition Differential Scanning Calorimetry (DSC) experiments (for cycles of heating and cooling) performed in controlled environments pre-conditioned to various relative humidities (RH) also indicated the presence of two distinct endothermal doublets. The endothermic peak temperatures were dependent on the RH and temperature history of the $Ca(OH)_2$ samples. An assessment of factors affecting the observed thermal behavior included: investigation of particle size and degree of crystallinity; observation of combined strain and particle size broadening (Williamson-Hall X-ray plots); heat capacity-temperature characteristics. A thermodynamic analysis of the thermal decomposition process is presented.

1. INTRODUCTION

The importance of $Ca(OH)_2$ in cement science is paramount. It occupies up to 26% by volume of hydrated Portland cement binders [1]. It is both a reaction product and a reactant. The well known hydration reactions associated with the silicate phases in Portland cement are the primary source. The $Ca(OH)_2$ is also a reactant with the various supplementary cements in widespread use e.g. fly ash, silica fume, slag and metakaolin [2]. Numerous studies have focused on the role of $Ca(OH)_2$ in sustainability issues related to concrete performance. Reactions that influence the durability of cement-based materials often involve $Ca(OH)_2$ [3].

Relatively recent applications of nanotechnology in cement science involve nanoparticulate or nanocomposite cement phases [4]. The focus of this work is the thermoanalytical characterization of nanoparticulate $Ca(OH)_2$. The presence of two distinct thermal decomposition events was detected for binary mixtures of $Ca(OH)_2$ polymorphs. Doublets in DTA curves of hydrated cements have been previously observed for the decomposition of $Ca(OH)_2$ by Greene and Herrick et al. [5, 6].

It is apparent that the characterization of nanomaterials in cement systems will become increasingly important. Results of an investigation to examine the thermal decomposition behavior of nano-sized $Ca(OH)_2$ particulates are presented. The influence of the degree of crystallinity and decomposition environment is examined. Thermodynamic arguments for the existence of distinct forms of $Ca(OH)_2$ and their thermal performance are given.

2. EXPERIMENTAL

2.1 Materials

CaO: Calcium oxide was prepared as described in Table 1.

Table 1: Preparation of CaO

	Preparation
CaO-1	Reagent grade $Ca(OH)_2$ was heated to 600°C and held isothermally for 1 hour. The nitrogen surface area of CaO-1 was 31.2 m^2/g.
CaO-2	Reagent grade $CaCO_3$ was heated to 1050°C and held isothermally for 1 hour. The nitrogen surface area of CaO-2 was 2.6 m^2/g.
CaO-3	Reagent grade $CaCO_3$ was heated to 1400°C and isothermally held for 1 hour. The nitrogen surface area of CaO-3 was 1.9 m^2/g.
CaO-4	Reagent grade $CaCO_3$ was heated at 1050°C and held isothermally for 3 hours. The nitrogen surface area of CaO-4 was 3.1 m^2/g.

$Ca(OH)_2$: Nine different samples of $Ca(OH)_2$ were prepared. The procedures are described in Table 2. The reagent grade $Ca(OH)_2$ was supplied by Anachemia Canada Inc., Montreal, Canada.

Table 2: Preparation of $Ca(OH)_2$ samples

Sample	Preparation
CH-1	CaO-1 was hydrated in an 11%RH environment for 7 days.
CH-2	CaO-1 was hydrated in deaerated water for 7 days.
CH-3	CaO-1 was hydrated in a 75%RH environment for 3 hours.
CH-4	Reagent grade $Ca(OH)_2$
CH-5	CaO-2 was hydrated in an 11%RH environment for 7 days
CH-6	CaO-2 was hydrated in deaerated water for 7 days.
CH-7	CaO-3 was hydrated in an 11%RH environment for 7 days.
CH-8	CaO-3 was hydrated in deaerated water for 7 days.
CH-9	CaO-4 was hydrated in deaerated water for 1 day.

$CaCO_3$: The reagent grade $CaCO_3$ was supplied by Anachemia Canada Inc., Montreal, Canada. The BET surface area was 2.6 m^2/g.

LiCl and NaCl: Reagent grade LiCl was supplied by Fisher Scientific, New Jersey, USA and NaCl by EMD Chemicals Inc., New Jersey, USA.

2.2 TG/DSC

A TA Instruments SDT-Q600 Thermal Analyzer was used for simultaneous TG and DSC measurements. A heating rate of 10°C/min (from room temperature to 1400°C) in a nitrogen gas environment (100mL/min) was employed. TG results are plotted in a derivative form (DTG). Heat flow data from the DSC measurements were used for heat capacity calculations.

The controlled environment DSC experiments employed a Dupont 1090 Thermal Analyzer used in conjunction with a DSC cell. A heating rate of 10°C with a nitrogen flow of 100 mL/min was used. The nitrogen was pre-conditioned at different values of RH, (12 – 100%). The nitrogen was passed over an aqueous salt solution at a predetermined RH. This was followed by flow into a vessel equipped with an RH sensor and through a flow meter into the DSC cell. It is noted that as the temperature in the DSC cell increases the saturation vapor pressure increases. The effective RH would therefore be less.

2.3 X-ray diffraction

A Scintag XDS 2000 instrument was used for X-ray diffraction measurements. CuK_α radiation (45 KV, 35 mA) was used. The scan rate was 0.025 degree/sec.

2.4 Surface area – BET method

Nitrogen surface area measurements were obtained with a Quantachrome Quantasorb Sorption System. Samples were dried at 140°C for 10 minutes prior to the measurements. The surface area values for the $Ca(OH)_2$ samples are given in Table 3.

Table 3: BET surface area values for various $Ca(OH)_2$ preparations

Sample	CH-1	CH-2	CH-3	CH-4	CH-5	CH-6	CH-7	CH-8	CH-9
Surface Area, m^2/g	20.1	31.1	21.5	16.6	3.7	7.3	5.1	7.8	6.5

3. RESULTS AND DISCUSSION

The presence of two separate and distinct thermal decomposition events in DTG and DSC experiments conducted with different $Ca(OH)_2$ preparations tested in environments conditioned at various RH was observed. The results are presented in three sections to illustrate the effect of degree of crystallinity, hydration environment and the underlying thermodynamic basis for the arguments advanced.

3.1 Effect of varying degree of crystallinity on thermal decomposition

The DTG curves for the vapor hydrated (CH-1, 11%RH) and liquid hydrated (CH-2) $Ca(OH)_2$ preparations are presented in Figure 1(a). Well defined doublets appear and are consistent with the relative proportions of each sample. The DTG results for CH-1 and CH-6 (liquid hydrated, lower surface area than CH-2) show similar trends, Figure 1(b). The vapor

hydrated CH-1 preparation had the lowest decomposition temperature. Characteristic doublets were also observed for binary mixtures of the vapor hydrated material (CH-3, 75%RH) and the high surface area material (CH-2), Figure 1(c). Similar behavior was observed for binary mixtures of vapor hydrated (CH-5, 11%RH) and liquid hydrated (CH-6) as well as for (CH-7, 11%RH) and liquid hydrated (CH-8), not shown.

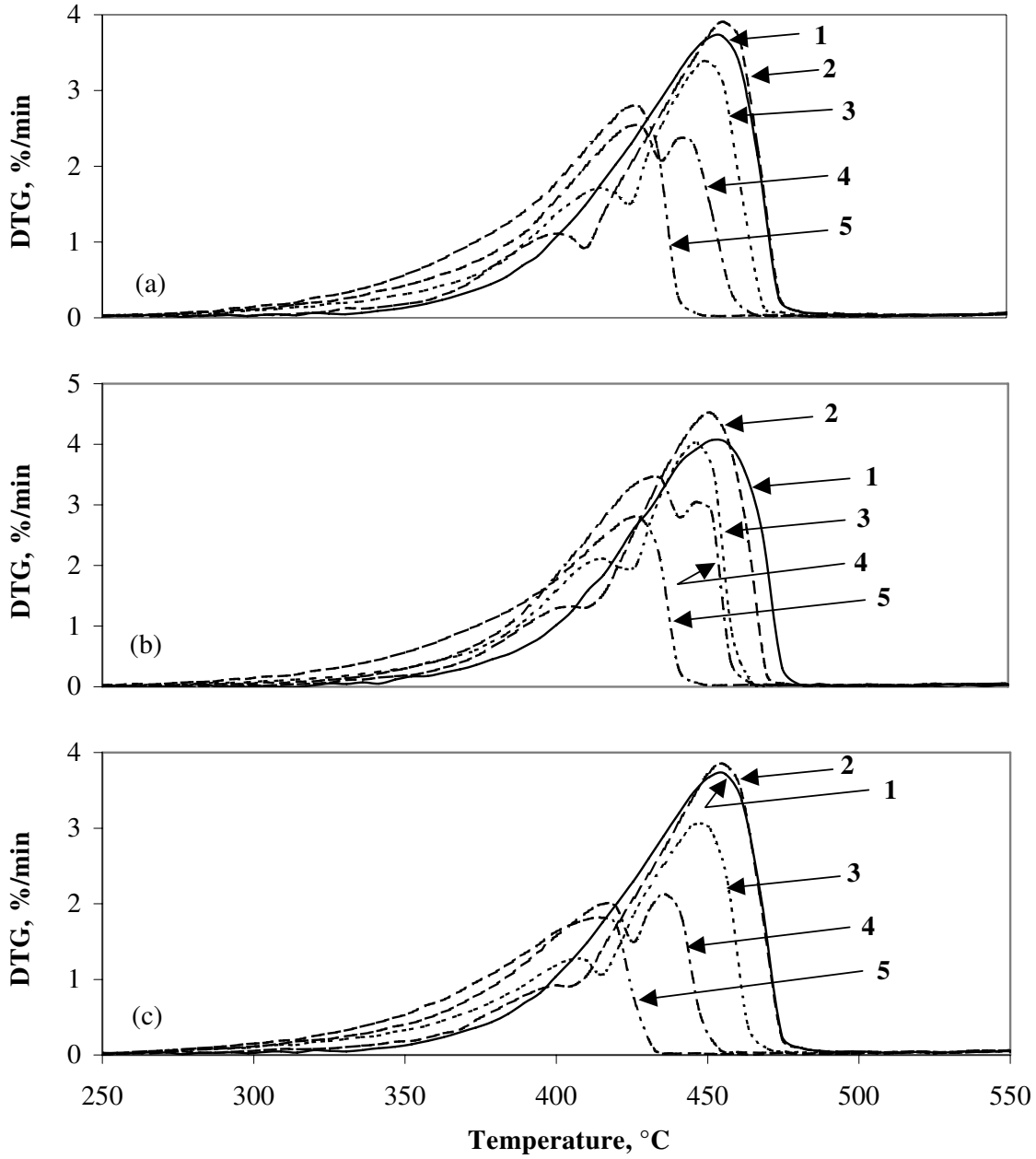

Figure 1: DTG curves for binary mixtures of $Ca(OH)_2$ polymorphs. Curves 1 – 5 refer to mixtures of (a) CH-1 and CH-2, (b) CH-1 and CH-6 and (c) CH-3 and CH-2. The content of CH-2, CH-6 and CH-2 respectively in (a), (b) and (c) for curves 1 – 5 is 100, 80, 50, 20 and 0%

Results of investigations on the effect of particle size on the decomposition temperature are often conflicting. Differences in fact may be due to variation in the degree of crystallinity [7]. For example, there appears to be no particle size effect for $Ca(CO)_3$ if the degree of crystallinity of the particles is similar [8]. Two methods were used to assess the relative differences in crystallinity of the $Ca(OH)_2$ preparations - calculation of a crystallinity index and Williamson-Hall analysis [9]. The index method utilizes the inverse of the peak width at half peak height (e.g. at $2\theta = 34.09°$) from the baseline as an indicator of the degree of crystallinity. Values of the crystallinity and thermal decomposition temperature support the view that the on-set of decomposition temperature is dependent on the degree of crystallinity (Table 4).

Table 4: Characterization data for selected $Ca(OH)_2$ preparations

Sample	BET, m^2/g	Crystallinity Index	Decomp. Onset, (1)	Decomp. Peak	Decomp. End, (2)	(2) – (1)
CH-1	20.1	1.72	231°C	426°C	467°C	236°C
CH-2	31.1	3.03	299°C	454°C	511°C	212°C
CH-6	7.3	5.26	308°C	452°C	512°C	204°C

The second method utilized the Williamson-Hall plots constructed from the X-ray data using Bruker AXS. TOPAS V2.1 Software [10]. It has been shown that line broadening can be attributed to simultaneous strain and small particle size broadening [9]. Plots of $B\cos\theta$ versus $\sin\theta$ are linear with the intercepts providing semi-quantitative values of the volume weighted characteristic length $\langle L \rangle_{vol}$ and the slopes indicating the level of lattice strain. The software enables the 'B' term to be extracted from the 'full width-half maximum' values (FWHM) of 'double-Voigt' fitting to the sample and the LaB_6 standard. The magnitude of the slopes of the lines and the degree of disorder are in the following order- CH-1> CH-2> CH-6- indicating that the lower decomposition temperature would be expected for the CH-1 preparation.

3.2 Effect of heating-cooling environment on thermal decomposition

The presence of at least two different forms of $Ca(OH)_2$ was confirmed by the results of DSC measurements performed in an atmosphere of a continuous flow of nitrogen pre-conditioned to various RH ranging from 12 to 100%. The $Ca(OH)_2$ sample CH-9 was selected for this study. On first heating it decomposes at higher temperatures as the RH of the environment increases, Figure 2(a). The $Ca(OH)_2$ decomposes more readily in the lower RH environments as the on-set of the endotherm and peak temperatures are reduced. The DSC curves that are typical of the re-heating curves after cooling are shown in Figure 2(b). The shift of the curves with RH is also observed. More well defined doublets also appear in the higher RH environments. The effect of cooling and re-heating on re-hydration and decomposition of the $Ca(OH)_2$ is illustrated in Figure 3. The CaO starts to re-hydrate at a higher temperature in the 100%RH environment. The range of the effective RH variation with temperature in the 100%RH cell (RH changes during the test due to non-equilibrium conditions) is much wider than for lower humidity conditions. This might be the reason for the more distinctive doublets in the 100%RH environment. Hydration of a sample produced in

different RH environments would result in a difference in degree of crystallinity and therefore a difference in decomposition temperature.

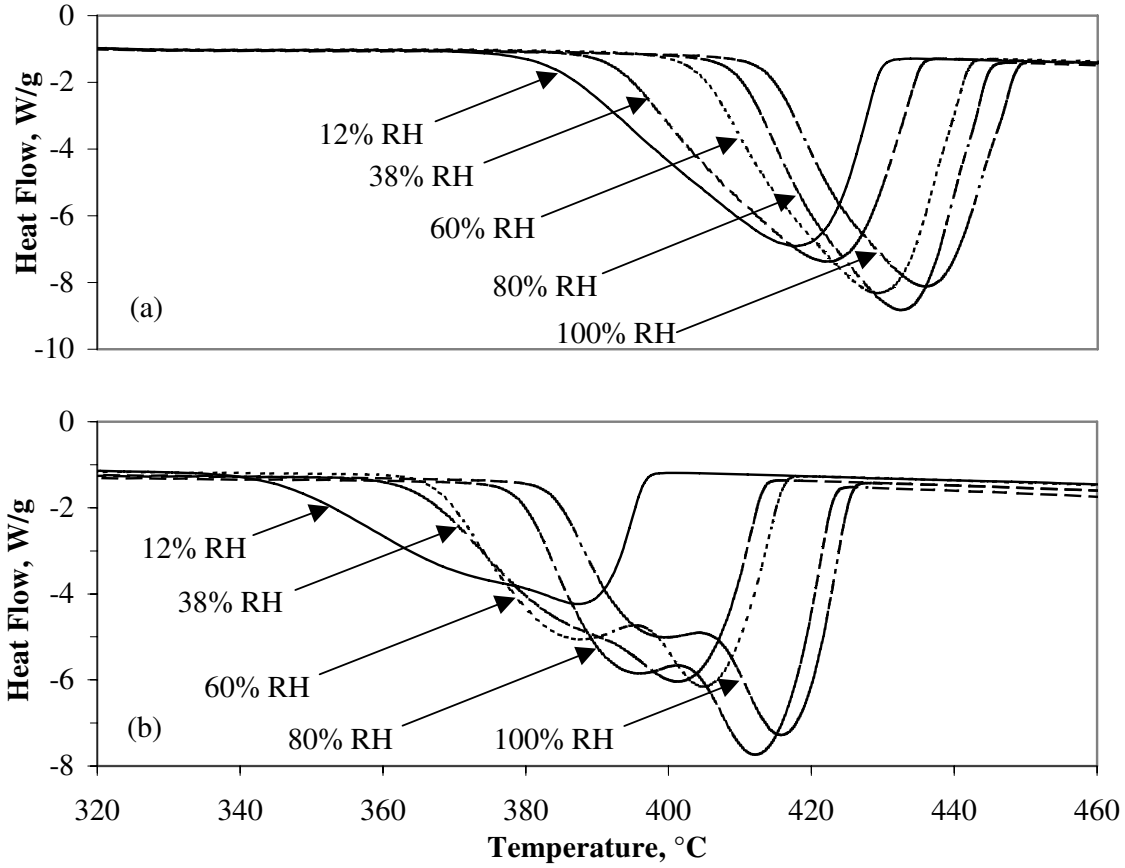

Figure 2: DSC curves for (a) 1st heating of CH and (b) re-heating after cooling in various RH environments

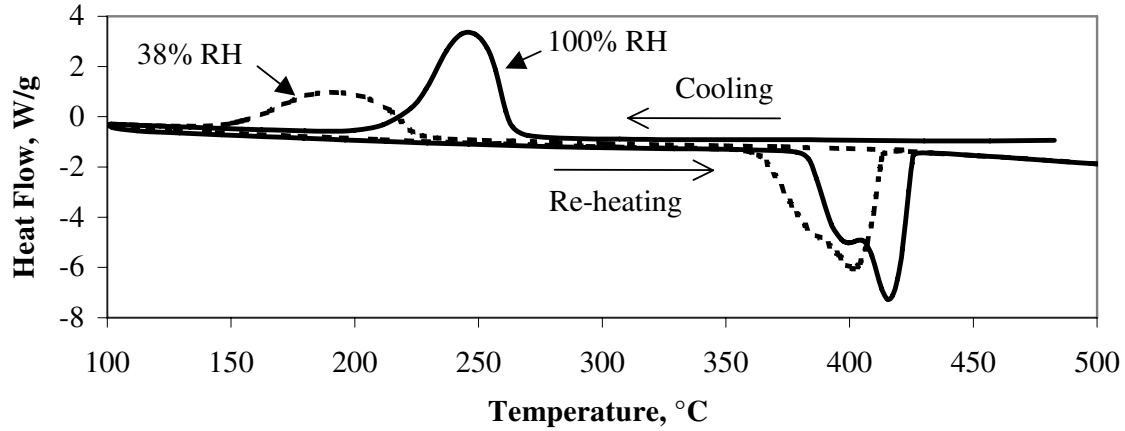

Figure 3: DSC curves for a typical cooling of CaO and re-heating of CH in a 38% and 100% RH environments

3.3 Thermodynamic analysis of the thermal decomposition of $Ca(OH)_2$

The following arguments are intended to support the previous discussion concerning the influence of the degree of crystallinity and the RH of the test environment on the thermal decomposition of $Ca(OH)_2$.

Heat capacity (C_p) - temperature functions were determined for selected $Ca(OH)_2$ preparations. The C_p values were calculated using the heat flow data obtained from the differential scanning calorimetry (DSC) results. They were calculated using the equation:

$$\left(\frac{Q}{m}\right) = C_p \cdot \left(\frac{\partial T}{\partial t}\right) = \left(W\, g^{-1}\right) = \left(J\, s^{-1}\, g^{-1}\right) = \left(J\, g^{-1}\, {}^{o}K^{-1}\right) \cdot \left({}^{o}K\, s^{-1}\right) \quad (1)$$

where, Q is the applied power (Watts or Joules per second),
m is the sample mass (grams),
C_p is the heat capacity (Joules per gram per degree Kelvin),
$\left(\frac{\partial T}{\partial t}\right)$ is the heating rate (degree Kelvin per second).

The curves were approximately linear in the temperature range, 350-500°, Figure 4. These functions can be used to estimate changes in enthalpy (ΔH) and entropy (ΔS) for each of the preparations. Generally,

$$\Delta H = \int_{T}^{T_1} C_p \partial T \text{ and } \Delta S = \int_{T}^{T_1} C_p / T \, \partial T \quad (2,3)$$

The determination of the change in Gibbs free energy can also be calculated from the general relationship:

$$\Delta G = \Delta H - T\Delta S \quad (4)$$

Hence, $\Delta G^{o}_{RT} = \Delta H^{o}_{RT} - T\Delta S^{o}_{RT}$ (at standard temperature and pressure) (5)

The decomposition temperature, T_d, of the CH specimens was calculated using Kirchoff's relationship. The enthalpy and entropy changes at any temperature were calculated utilizing the enthalpy and entropy changes at the standard condition and the heat capacities of the reactants and products in the range of temperatures under consideration. The Kirchoff's relationship was represented as:

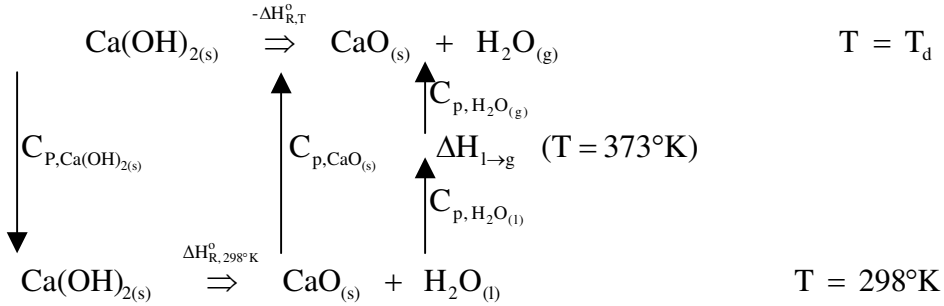

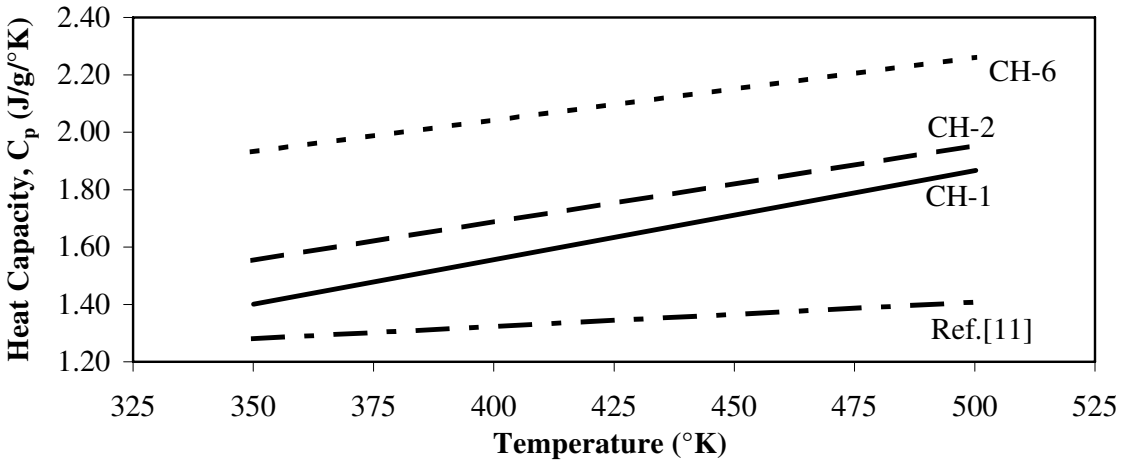

Figure 4: Region of Linear Temperature Dependence for Heat Capacity Values of CH Polymorphs

The standard enthalpy of reaction at 298°K was calculated from tabulated values for the enthalpy of formation of the reactants and products.

$$\Delta H^{o}_{R,298K} = \Delta H^{o}_{f,CaO_{(s)}} + \Delta H^{o}_{f,H_2O_{(l)}} - \Delta H^{o}_{f,Ca(OH)_{2(s)}} \quad (6)$$

$= -151{,}600 - 68{,}315 - (-235{,}500) = 15{,}585$ calories mol^{-1}

The heat required to bring $CaO_{(s)}$ from 298°K to a higher temperature T is:

$$\Delta H_1 = \int_{298}^{T} C_{p,CaO_{(s)}} \partial T \quad (7)$$

$= \Phi_1(T)$ cal mol^{-1}

Similarly for $H_2O_{(l)}$ taking into account the phase transition at 373°K:

$$\Delta H_2 = \int_{298}^{373} C_{p,H_2O_{(l)}} \partial T + \Delta H_{l \to g} + \int_{373}^{T} C_{p,H_2O_{(g)}} \partial T \quad (8)$$

$= \Phi_2(T)$ cal $mole^{-1}$

Now $C_{p,Ca(OH)_{2(S)}} = a + bT$ cal mol^{-1} $^{\circ}K^{-1}$

The enthalpy released as $Ca(OH)_2$ is brought from T to 298°K is:

$$\Delta H_3 = \int_{T}^{298} C_{p,Ca(OH)_{2(s)}} \partial T \quad (9)$$

$= \Phi_3 (a, b, T)$ cal.mol^{-1}

Using Kirchoff's relationship:

$$\Delta H^{o}_{R,298K} + \Delta H_1 + \Delta H_2 - \Delta H^{o}_{R,T} + \Delta H_3 = 0 \quad (10)$$

Substituting for these quantities and simplifying yields:

$$\Delta H^{o}_{RT} = \Phi_4 \text{ (a,b,T)} \quad (11)$$

Entropies can be calculated similarly leading to the following:

$$\Delta S_{RT}{}^{o} = \Phi_5 \text{ (a, b, T) cal mol}^{-1}\ ^{\circ}\text{K}^{-1} \quad (12)$$

The Gibbs free energy for the decomposition reaction is determined from:

$$\Delta G^{o}_{R,T} = \Delta H^{o}_{R,T} - T\Delta S^{o}_{R,T} \quad (13)$$

$= \Phi_6$ (a, b, T) following previous arguments.

The generalized form is:

$$\Delta G_{R,T} = \Delta G^{o}_{R,T} + RT \ln\left(\frac{a_{CaO_{(s)}} \cdot P_{H_2O_{(g)}}}{a_{Ca(OH)_2}}\right) \quad (14)$$

where $a_{CaO_{(s)}}$ and $a_{Ca(OH)_{2(s)}}$ are the activities of CaO and $Ca(OH)_2$, respectively, and $P_{H_2O_{(g)}}$ is the normalized partial pressure of water vapor. R is the universal gas constant given as 1.987 calories mol^{-1} K^{-1}. With the appropriate substitutions, the generalized Gibbs free energy of reaction is,

$$\Delta G_{RT} = \Phi_7 \text{ (a, b, T, } P_{H2O(g)}) \text{ cal.mol}^{-1} \quad (15)$$

The temperature at which ΔG_{RT} is zero corresponds to the decomposition temperature of $Ca(OH)_2$, T_d. It can be seen that T_d depends on the RH condition and the C_p temperature dependence for the $Ca(OH)_2$ samples prepared under different conditions. The heat capacity (C_p) results are summarized in Table 5.

Table 5: Heat capacities of $Ca(OH)_{2(s)}$ prepared under different conditions

Preparation	Heat Capacity (a + bT)			
	$J\ g^{-1}\ K^{-1}$		$Calories\ mol^{-1}\ K^{-1}$	
	a	b	a	b
CH-1	0.3136	0.0032	5.55	5.489×10^{-2}
CH-2	0.6204	0.0027	10.99	4.781×10^{-2}
CH-6	1.1654	0.0022	20.64	3.896×10^{-2}
Reference Values – Linear Approximation (Ref. [11])	0.9811	0.0009	17.37	1.594×10^{-2}

The normalized water vapor partial pressures for 11%, 75%, and 100% RH and for the standard state (i.e. 101.3 kPa) are given in Table 6.

Calculated values for the on-set of the decomposition temperature T_d are given in Table 7. The decomposition temperature of CH for all preparations increases as the humidity in the decomposition environment increases. Further the $Ca(OH)_2$ prepared by liquid phase hydration decomposes at higher temperatures than the $Ca(OH)_2$ prepared by vapor hydration suggesting that the liquid hydrated samples are more thermodynamically stable than the vapor hydrated samples.

Table 6: Experimental humidity conditions

Condition	Normalized Pressure (P_i / 101.6 kPa)
11%RH	0.0034
75%RH	0.0235
100%RH	0.0313
Standard State	1

Table 7: Calculated decomposition temperatures, T_d (^oC) for $Ca(OH)_2$

Normalized H_2O (g) Pressure	Vapor Hydrated Preparations	Liquid Hydrated Preparations		Using Reference Values (Ref. [11])*
	CH-1	CH-2	CH-6	
Dry Nitrogen	301	320	334	-
0.0034	311	318	338	303
0.0235	374	386	422	359
0.0313	385	398	438	368
1	582	626	925	514

* The preparation procedure for the $Ca(OH)_2$ used in Ref. [11] was unspecified.

4. CONCLUSIONS

- $Ca(OH)_2$ preparations of varying crystallinity can be produced by employing vapor phase and liquid phase hydration of CaO.
- Two or more distinct forms of $Ca(OH)_2$ with separate thermal decomposition temperatures (endothermal doublets) can easily be produced.
- Thermal decomposition temperatures of $Ca(OH)_2$ appear to be related more to the degree of crystallinity than to surface area or particle size.
- Thermograms for the decomposition of $Ca(OH)_2$ indicate the presence of two distinct forms (reflected by two endotherms) when the decomposition and re-hydration process occur in a controlled humidity and CO_2 free environment.
- The magnitude of both the low and high temperature endothermic peak heights is dependent on the relative humidity and temperature in a DSC test environment.
- Higher temperature is conducive to formation of a more crystalline $Ca(OH)_2$ product, while at the same time, vapor phase hydration promotes formation of a microcrystalline product.
- The thermodynamic analysis corroborates the validity of the previously observed doublets in the thermal analytical spectral information (DTG, DSC) for $Ca(OH)_2$.
- Thermodynamic calculations of the decomposition temperature of $Ca(OH)_2$ support previous arguments that $Ca(OH)_2$ with varying degrees of crystallinity can be produced.
- The observations that the decomposition temperature of the various $Ca(OH)_2$ preparations increases as the relative humidity of the environment under which decomposition occurs increases and that it is dependent on the degree of crystallinity of the $Ca(OH)_2$ are compatible with thermodynamics – based arguments.

ACKNOWLEDGEMENTS

The authors would like to thank Mr. Gary Polomark for conducting many of the experiments.

REFERENCES

[1] Taylor, H.F.W., 'Cement Chemistry', 2nd Edn. (Thomas Telford, London, 1997).
[2] Malhotra, V.M., Ramachandran, V.S., Feldman, R.F. and Aitcin, P.C., 'Condensed Silica Fume in Concrete', (CRC Press Inc., Boca Raton, Florida, 1987).
[3] Glasser, F.P., 'The role of $Ca(OH)_2$ in Portland cement concretes', in Materials Science of Concrete - Special Volume: Calcium Hydroxide in Concrete, **6**, Eds. J. Skalny, J. Gebauer, J. Odler, (Amer. Ceram. Soc., 2001) 11-36.
[4] Raki, L., Beaudoin J.J., Mitchell L.D., 'Layered double hydroxide-like materials: nanocomposites for use in concrete', *Cem. Concr. Res.* **34** (2004), 1717-1724.
[5] Green, K.T., 'Early hydration reactions of Portland cement', in Proceedings 4th International Congress on Chem. of Cem., Washington DC, 1960, Vol. I, Session IV, Paper IV-1, 359-374.
[6] Herrick, J., Scrivener K. and Pratt P., 'The development of microstructure in calcium sulphoaluminate expansive cement', in Proceedings Matls. Res. Soc., Vol. 245 (1992) 277-282.
[7] Tanaka, T., 'Simultaneous grinding and reaction', *Minerals Process*, **5** (1964) 31.
[8] Bayliss, P., 'Effect of particle size on differential thermal analysis', *Nature*, **201**, (1964) 1019.
[9] Williamson G.K. and Hall W.H.,'X-ray line broadening from filed aluminium and wolfram', *Acta Metallurgica*, **1** (1953) 22-31.
[10] Bruker AXS.TOPAS V2.1 User Manual, Karlsruhe Germany (2003).
[11] Kubaschewski, O. and Alcock, C.B., 'Metallurgical Thermochemistry, 5th Edn., (Pergamon Press, Toronto, 1979).